# Hybrid Uranyl-Carboxyphosphonate Cage Clusters

Pius O. Adelani,[†] Michael Ozga,[†] Christine M. Wallace,[†] Jie Qiu,[†] Jennifer E. S. Szymanowski,[†] Ginger E. Sigmon,[†] and Peter C. Burns*[†,‡]

[†]Department of Civil and Environmental Engineering and Earth Sciences and [‡]Department of Chemistry and Biochemistry, University of Notre Dame, Notre Dame, Indiana 46556, United States

S *Supporting Information*

ABSTRACT: Two new hybrid uranyl-carboxyphosphonate cage clusters built from uranyl peroxide units were crystallized from aqueous solution under ambient conditions in approximately two months. The clusters are built from uranyl hexagonal bipyramids and are connected by employing a secondary metal linker, the 2-carboxyphenylphosphonate ligand. The structure of cluster **A** is composed of a ten-membered uranyl polyhedral belt that is capped on either end of an elongated cage by five-membered rings of uranyl polyhedra. The structure of cluster **B** consists of 24 uranyl cations that are arranged into 6 four-membered rings of uranyl polyhedra. Four of the corresponding topological squares are fused together to form a sixteen-membered double uranyl pseudobelt that is capped on either end by 2 topological squares. Cluster **A** crystallizes over a wide pH range of 4.6−6.8, while cluster **B** was isolated under narrower pH range of 6.9−7.8. Studies of their fate in aqueous solution upon dissolution of crystals by electrospray ionization mass spectrometry (ESI-MS) and small-angle X-ray scattering (SAXS) provide evidence for their persistence in solution. The well-established characteristic fingerprint from the absorption spectra of the uranium(VI) cations disappears and becomes a nearly featureless peak; nonetheless, the two compounds fluoresce at room temperature.
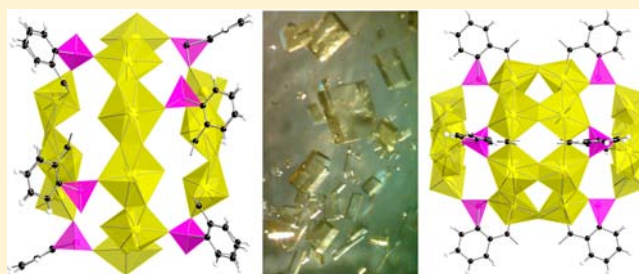
INTRODUCTION

The development of new synthetic strategies to assemble uranyl peroxide clusters with unique topologies and tunable properties is presently a key goal in the field of nanostructure actinide chemistry. To date, over 35 notable actinide peroxide clusters have been synthesized in aqueous solution under ambient conditions.[1−20] Burns and his co-workers have demonstrated that uranyl peroxide clusters can be extended significantly through the incorporation of different anions such as nitrate, oxalate, phosphate, and phosphonates.[8−10,13,15,17] Most of the earlier investigations in this area of study were centered on the synthesis and structures of actinide clusters, and future research efforts on their properties and applications hold considerable promise. However, because of the radioactivity of actinides, their applications are likely to differ from those of transition metal polyoxometalates. Notwithstanding, actinide peroxide clusters are inspiring the development of new techniques in advanced nuclear energy systems such as mass-based separations of used nuclear fuel and materials fabrication, as well as models for actinide transportation in the environment.[2,12,19,20]

In the past two decades, several research groups have shown that actinide atoms can be incorporated in heteropolytungstates for use in sequestration and storage of actinide waste.[21−30] Further studies have examined the incorporation of uranyl peroxo in polyoxotungstates, thus inspiring their use as potential candidates in the design of catalysts.[31−33] Phosphonate derivatives are pliable and have proven to be a ligand of choice to introduce curvature in structural units containing uranyl polyhedra.[34,35] The different binding preferences of the bifunctional 2-carboxyphenylphosphonate ligand allow for the construction of heterobimetallic U(VI)-3d complexes.[36] When nickel metal ions are incorporated in the structure of uranyl carboxyphosphonate, a remarkable heteropolyoxometalate structure results: $[H_3O]_4[Ni(H_2O)_3]_4\{Ni[(UO_2)-(PO_3C_6H_4CO_2)]_3(PO_4H)\}_4 \cdot 2.72H_2O$.[37]

Our current research efforts are focused on incorporating organic moieties as linkers in the design of uranyl peroxide cage clusters to vastly expand their structural topologies, properties, and functions. Herein, we report the synthesis, structural characterization, and spectroscopic properties of two hybrid uranyl-carboxyphosphonate cage clusters, (**A**) and (**B**).

EXPERIMENTAL SECTION

Synthesis. *Caution! While the uranium used in these studies was isotopically depleted, precautions are needed for handling radioactive materials, and all studies should be conducted in a laboratory dedicated to studies of toxic and radioactive materials.*

Distilled and Millipore filtered water with a resistance of 18.2 MΩ cm was used in all reactions.

2-Carboxyphenylphosphonic acid (2-CPPA). Diethyl (2-ethoxycarbonylphenyl)phosphonate (96%, Epsilon Chimie) was dissolved in 20 mL of concentrated hydrochloric acid and allowed

to reflux for 24 h. The white crystals of 2-carboxyphenylphosphonic acid (2-CPPA) formed during cooling to room temperature. The crystals were filtered and dried in an oven at 60 °C.

$[K_{18}Li_{12}][(UO_2)_{20}(HO_2CC_6H_4PO_3)_{10}(O_2)_{20}(OH)_{10}](H_2O)_n$ (A) and $[K_3Li_{21}[(UO_2)_{24}(HO_2C-C_6H_4PO_3)_8(O_2)_{24}(OH)_8](H_2O)_n$ (B). Crystals of **A** were synthesized by loading a mixture of solutions containing $UO_2(NO_3)_2 \cdot 6H_2O$ (0.5 M, 0.1 mL), H_2O_2 (30%, 0.1 mL), LiOH (2.4 M, 0.1 mL), KCl (0.5M, 0.1 mL), and 2-CPPA (0.25 M, 0.2 mL) in a 4 mL scintillation vial with initial pH ranging over 4.8−6.8. The resulting solution was left standing opened to air to permit slow evaporation, and yellow tablets of **A** appeared after approximately two months (yield: 44% on the basis of uranium). Yellow crystals of **B** were isolated, along with fine-grained yellow precipitates that we have been unable to identify, by slightly modifying a mixture of the solution above. We increased the pH slightly with LiOH (2.4 M, 0.12 mL) and reduced the concentration of KCl (0.5 M, 0.05 mL) to minimize the precipitates formed. The initial pH values ranged from 6.9−7.8 (yield: ~10% on the basis of uranium).

Crystallographic Studies. A single crystal of each of the compounds was mounted on a cryoloop and optically aligned on a Bruker APEX II Quazar CCD X-ray diffractometer using a digital camera. Initial intensity measurements were performed using a IμS X-ray source and a 30 W microfocused sealed tube (Mo Kα, λ = 0.71073 Å) with a monocapillary collimator. Semiempirical corrections for absorption were applied to the full sphere of data collected in each case using the program SADABS. Data were integrated using the Bruker APEX II software, and the SHELXTL system of programs was used for the solution and refinement of each structure.[38] Refinement of crystal structures such as these that contain cage clusters built from uranyl polyhedra is particularly challenging because of the X-ray scattering dominance of uranium as compared to the lighter atoms (i.e., H, C, and O), the presence of relatively large voids with little electron density, and disorder of counterions and water molecules. These factors result in relatively weak and poor diffraction at higher angles, and limit the resolution of the crystal structure. Soft constraints were added to the refinements in this study to improve the geometries of the disordered counterions and lighter elements. Despite the shortcomings of X-ray diffraction for studying such structures, the method provides definitive details of many aspects of the structures. Lithium cations are especially difficult to locate and may be mostly disordered. Chemical analyses and charge-balancing considerations provide further details of the formula for the crystals studied. Selected crystallographic data are presented in Table 1. Atomic coordinates, bond distances, and additional structural information are provided in the crystallographic data (CIF).

Elemental Analysis. To confirm the presence of U, P, K, and Li cations, crystals of each of the compounds were washed lightly with deionized water under vacuum and were subsequently dissolved for analysis using a PerkinElmer ICP-OES. Energy dispersive spectra (EDS/EDX) were collected for single crystals corresponding to each cluster using a LEO EVO-50XVP variable-pressure/high-humidity scanning electron microscope. Spectra collected for each compound confirmed the presence of U, P, and K for **A** and **B**, respectively, consistent with the results from ICP-OES which also confirmed the presence of Li cations.

Small-Angle X-ray Scattering. Small-angle X-ray scattering (SAXS) data were collected using a Bruker Nanostar equipped with a Cu microfocus source, Montel multilayer optics, and a HiSTAR multiwire detector. Data were collected with the sample chamber under vacuum and a sample-to-detector distance of 26.3 cm. Crystals were first isolated from their mother solution by vacuum filtration. They were rinsed gently using water and were then harvested from the filter membrane prior to dissolution in ultrapure water. The resulting solutions were drawn into 0.5 mm diameter glass capillaries, and the ends of each capillary were sealed using wax. Water in an identical capillary was used for background measurement.

Electrospray Ionization Mass Spectrometry. ESI-MS spectra were collected in negative-ion mode using a Bruker micrOTOF-Q II high-resolution quadrupole time-of-flight (Q-TOF) spectrometer (3600 V capillary voltage, 0.8 bar nebulizer gas, 4 L/min dry gas,

Table 1. Crystallographic Data for A and B

	cluster **A**	cluster **B**
formula mass	9354.88	9582.60
color and habit	yellow, tablet	yellow, tablet
space group	$P2_1/c$ (No. 14)	$C2/c$ (No. 15)
a (Å)	17.975(3)	35.433(3)
b (Å)	34.567(5)	24.290(2)
c (Å)	21.848(3)	32.991(1)
α (deg)	90	90
β (deg)	102.498(2)	104.549(1)
γ (deg)	90	90
V (Å)	13253(4)	27484(4)
Z	2	4
T (K)	100	100
λ (Å)	0.71073	0.71073
ρ_{calcd} (g cm^{-3})	2.344	2.316
μ (Mo Kα) (mm^{-1})	12.605	14.263
$R(F)$ for $F_o^2 > 2\sigma (F_o^2)^a$	0.065	0.074
$Rw(F_o^2)^b$	0.208	0.247

$^aR(F) = \sum ||F_o| - |F_c||/\sum|F_o|.$ $^bR(F_o^2) = [\sum w(F_o^2 - F_c^2)^2/\sum w(F_o^4)]^{1/2}.$

180 °C dry gas temperature). The samples were introduced by direct infusion at 7 μL/min and scanned over the range m/z 500−5000 with data averaged over 5 min. The data were deconvoluted using MaxEnt software.[39]

Spectroscopic Properties. Absorption and fluorescence data were acquired from a single crystal of each compound using a Craic Technologies UV−vis−near-IR (NIR) microspectrophotometer with a fluorescence attachment. The absorption data were collected in the range of 250−1200 nm at room temperature. Excitation was achieved using 365 nm light from a mercury lamp for the fluorescence spectroscopy. The IR spectra were collected from single crystals of **A** and **B** using a SensIR Technology IlluminatIR FT-IR microspectrometer. A single crystal of each compound was placed on a glass slide and the spectrum was collected with a diamond ATR objective.

■ RESULTS

Structure of $[K_{18}Li_{12}][(UO_2)_{20}(HO_2CC_6H_4PO_3)_{10}(O_2)_{20}(OH)_{10}](H_2O)_n$ (A). The X-ray crystal structure analysis provided the formula $\{[K_{18}Li_4][(UO_2)_{20}(HO_2CC_6H_4PO_3)_{10}(O_2)_{20}(OH)_{10}](H_2O)_n\}^{8-}$, and the remaining charge is presumably balanced by K$^+$ and Li$^+$ cations that are located within or between the cage clusters. The structure contains considerable electron density that we attribute to unassigned disordered Li$^+$ and H$_2$O molecules. SQUEEZE was applied to the data to confirm that a 3,588 Å^3 void contains about 2,380 electrons. ICP-OES analyses indicate 18 K$^+$ and 12 Li$^+$ cations per formula unit; 8 Li$^+$ cations were not assigned in the crystal structure presumably because of their weak X-ray scattering.

The overall structure of **A** consists of 20 uranyl hexagonal bipyramids and 10 carboxyphosphonate groups, forming nanoscopic cage clusters approximately 13.7 × 18.1 Å in diameter, as measured from the outer oxygen atoms of the uranyl cations (see Figure 1a, b). The basic uranyl diperoxide hexagonal bipyramidal units are arranged in two patterns: 2 five-membered uranyl rings are positioned at either end of the cage as shown in Figure 2a, and the remaining uranyl cations are assembled into a rare ten-membered uranyl belt (see Figures 2b and 3a). These two distinct uranyl arrangements are loosely linked through the carboxyphosphonate moiety. Topological pentagons are common graphical representations
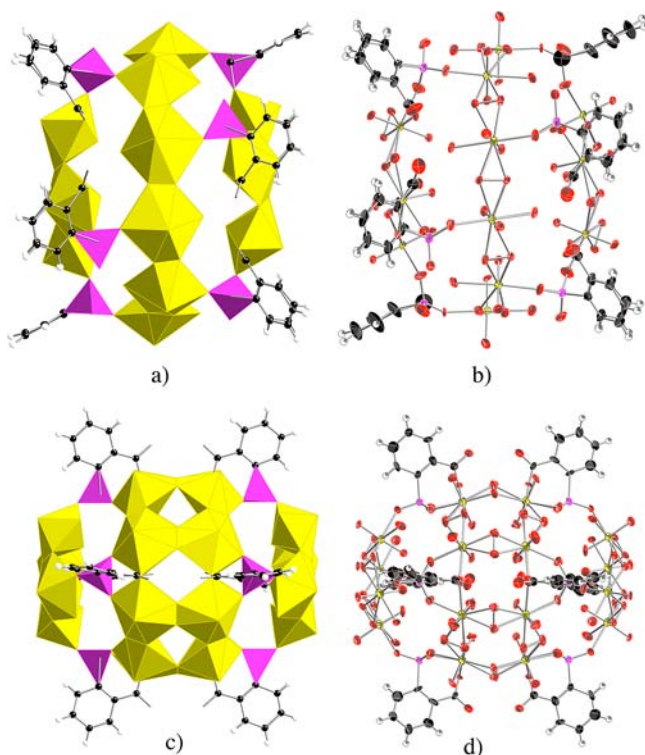
Figure 1. Polyhedral representations and ellipsoid diagrams of **A** (a, b) and **B** (c, d). UO_8 units = yellow, phosphorus = magenta, oxygen = red, carbon = black, hydrogen = white. Ellipsoids are shown at the 50% probability level.
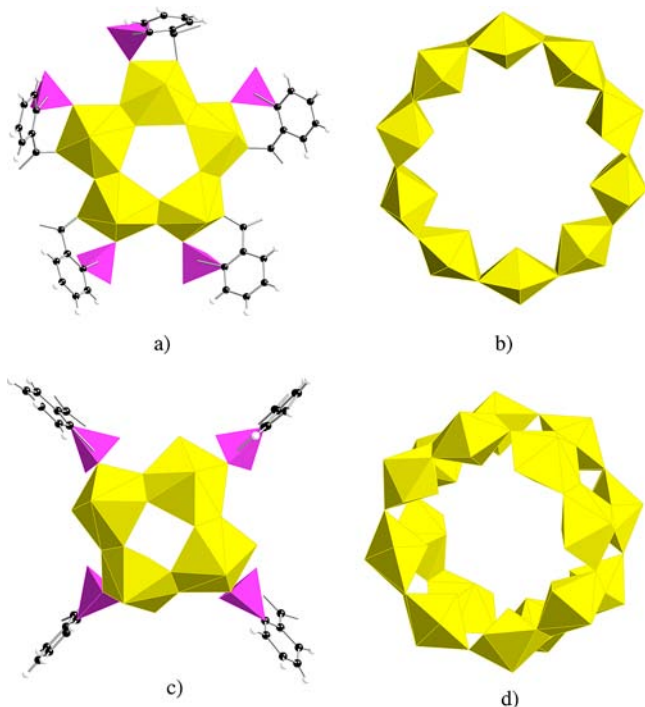

Figure 2. Comparison of structural fragments from **A** (a,b) and **B** (c,d) clusters. These fragments correspond to topological pentagons (a) and the 10-membered uranyl belt in **A**, squares and fused squares in **B** (c,d). Legend as in Figure 1.

in uranyl peroxide clusters. Uranyl belts are rare, and the side-by-side arrangement pattern we reported herein is distinct from
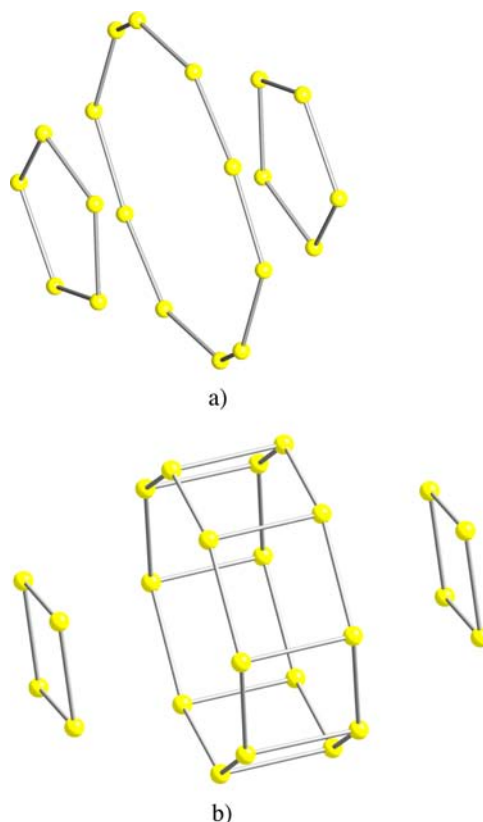

Figure 3. Connectivity diagrams in **A** (a) and **B** (b), the yellow nodes represent uranyl atoms and links indicate connections between them.

all other patterns that have been reported in crystal structures.[13,15,18] In uranyl peroxide pyrophosphate/phosphate cage clusters, uranyl belts are arranged in a zigzag pattern to accommodate the coordinated pyrophosphate/phosphate moieties.[13,15] The fragments of uranyl belts from the recently reported chiral uranyl peroxo cage clusters are built from only four uranyl cations.[18]

All the uranium centers in **A** are coordinated by two nearly linear oxo atoms, forming a classical uranyl ion, UO_2^{2+} unit, and the O−U−O bond angles range from 177.8(5) ° to 179.6(5) ° with normal U−O bond distances that range from 1.765(11) Å to 1.819(10) Å. Six oxygen atoms are coordinated to the uranyl cations at the equatorial vertices of hexagonal bipyramids with U−O bond distances that range from 2.288(12) to 2.522(11) Å; the longer U−O bond lengths reveal the presence of hydroxyl groups. The equatorial ligands for the uranyl cations consist of two bidentate peroxide groups, with the remaining two O_2 atoms from phosphonate-carboxylate groups and phosphonate-hydroxyl groups for the five and ten-membered rings, respectively. The calculated bond-valence sums for the uranyl cations and the absorption spectrum (see Figure 5) are consistent with the formal valence of U(VI).[40,41] The P−O bond lengths from the phosphonate groups range from 1.507(11) Å to 1.562(12) Å. The phenyl ring bearing the P(1) atom is disordered; therefore, the bond lengths from the P(1) atom are outside the normal range. The C−O bonds within the carboxylate moiety range between 1.209(19) and 1.420(20) Å. Atom C(7) is also disordered, and the C−O bond lengths are not included within the above bond distance values. The protonation of the C−O group is indicative of the terminal and slightly elongated C−O bonds.

Structure of $[K_3Li_{21}][(UO_2)_{24}(HO_2CC_6H_4PO_3)_8(O_2)_{24}$-$(OH)_8](H_2O)_n$ (B). The X-ray crystal structure analysis supports the formula $[K_3][(UO_2)_{24}(HO_2CC_6H_4PO_3)_8(O_2)_{24}(OH)_8]$-$(H_2O)_n\}^{21-}$, with disordered electron density within and between the cage clusters left unassigned. SQUEEZE was applied to the data to confirm that a 10,717 Å^3 void contains about 5,857 electrons. We attribute the unassigned electron density to disordered Li$^+$ and H$_2$O molecules. Atomic percentages for U, P, and K from EDX analysis are consistent with the result from the X-ray diffraction. The X-ray scattering is ineffective for locating Li atoms in the crystal structure; therefore ICP-OES analyses are necessary. The ratios of the U/P/K/Li atoms varied slightly as a result of difficulties we encountered in separating the crystals from the unidentified fine-grained yellow precipitates formed. This prompted us to assume that the remaining 21 electrons are balanced with Li$^+$ cations, since all the K$^+$ ions have been accounted for through the single crystal X-ray solution.

The cluster **B** is topologically divergent from **A** in that there are 8-membered uranyl double rings positioned at the middle of the elongated cage which is capped at either end by 2 four-membered uranyl rings (see Figure 1c and d). The cage is approximately 13.4 × 17.9 Å in diameter, as measured from the outer oxygen atoms of the uranyl cations. Only one unique coordination arrangement is formed around the uranyl cations: 2 four-membered uranyl rings (see Figures 2c and 3b), and the remaining sixteen uranyl cations are assembled into 4 four-membered uranyl rings that are fused together through the carboxylate groups into uranyl pseudobelts as shown in Figure 2d.

The 24 uranium cations are each part of a typical UO$_2^{2+}$ unit, with an average O−U−O bond angle of 177(8)° and U−O bond length of 1.783(15) Å. The equatorial ligands consist of two bidentate peroxide groups, one oxygen from the phosphonate and one hydroxyl group for each uranyl ion within the four-membered uranyl ring. The sixteen uranyl cations of the fused four-membered ring are coordinated to two O$_2$ atoms from phosphonate and carboxylate moieties, along with the four oxygen atoms of the two bidentate peroxide groups. The calculated bond-valence sums at the uranium centers and the absorption spectrum are in agreement with U(VI) (see Figure 5).[40,41] The P−O and C−O bond lengths from the phosphonate and carboxylate moieties are within the ranges observed in **A**.

SAXS and ESI-MS Studies of Dissolved A and B. Characterization of the clusters in solution was performed using SAXS and ESI-MS to probe their behavior in ultrapure water. The radius of gyration, R_g, of the macroions in solution was determined using Guinier analysis of the very low angle scattering data.[42] The value of R_g derived from the data (see SAXS Supporting Information, Figure S1) was found to be 7.7 and 7.4 Å for **A** and **B**, respectively; these are comparable to the estimated experimental values derived from the crystallographic data, 7.9 and 7.8 Å, respectively, for **A** and **B**. The ESI-MS data are shown in Figure 4 and are highly reproducible. Data for **A** and **B** were deconvoluted using the MaxEnt software. Data from a dissolved single crystal of compound **A** was collected on the same day that the solution was prepared, and although the cluster was still present, other species present indicated partial disintegration, either in solution or in the spectrometer. The assignment of charge state from the isotopic separation reveals −6 (m/z 1290), −5 (m/z 1552), and −4 (m/z 1945), yielding an average formula weight of 8004 D. The ESI-MS data of **A**
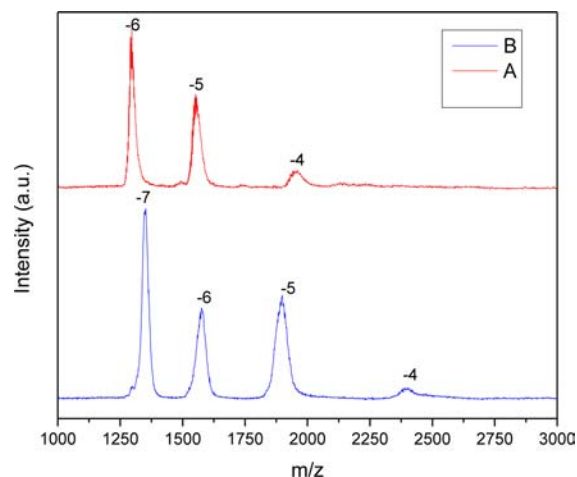

Figure 4. ESI-MS data for samples made by dissolving single crystals of **A** and **B** in ultrapure water.

after day 1 indicated the presence of an additional species in solution. Therefore, we investigated further by slowly evaporating the solution of **A**. Crystals of uranyl peroxide clusters containing the common U24 cluster were isolated. The deconvolution of the ESI-MS data collected from the solution of **B** in ultrapure water gave an average mass of 9701 Da, and its assigned charge states from the isotopic separation reveals −7 (m/z 1347), −6 (m/z 1578), −5 (m/z 1902), and −4 (m/z 2404).

Spectroscopic Properties. The UV−vis−NIR absorption spectra for uranyl(VI) complexes [i.e., the benchmark compound, $UO_2(NO_3)_2\cdot6H_2O$] contain the characteristic equatorial U−O charge transfer bands of uranyl centered at 325 nm, as shown in the Figure 5. In addition, the axial U−O charge transfer bands are observed around 421 nm with a characteristic vibronic fine-structure. The absorption spectrum from a single crystal of **A** is similar to that of **B** and their spectra are comparable to those of reported uranyl peroxide clusters.[16,18] The characteristic fingerprint of uranyl nitrate hexahydrate is not evident, instead there is a relatively broad spectrum that is almost a featureless peak from 300 to 550 nm. The spectra reveal a shoulder around 354 nm and a distinct peak around 416 nm. The loss of the fine structure in the absorption spectra of uranyl peroxide clusters and the significantly higher molar absorptivity are presumably due to the intense ligand-to-metal charge transfer between coordinated peroxide and the uranyl(VI) moiety and the resulting bent configuration of the U-(O$_2$)-U moiety (asymmetric molecules).[43,44] It has also been well established that most uranyl-containing compounds emit green light centered near 520 nm. The charge-transfer-based emission is in fact vibronically coupled to both bending and stretching modes of the uranyl cation, yielding a well resolved five-peak pattern at room temperature.[45] We and others have shown that luminescent properties can be enhanced by stronger metal-to-aromatic ligand interactions from carboxyphosphonates and pyridinedicarboxylates.[46,47] Despite the loss of vibronic fine-structure in the absorption spectra of uranyl peroxide clusters, intense emission with vibronic coupling are clearly observed in the fluorescence spectra of compounds **A** and **B** (see Figure 6). The two uranyl-carboxyphosphonate cage clusters reveal four peaks that are clearly resolved at 488, 543, 585, and 611 nm. These clusters are red-shifted by approximately 34 nm relative
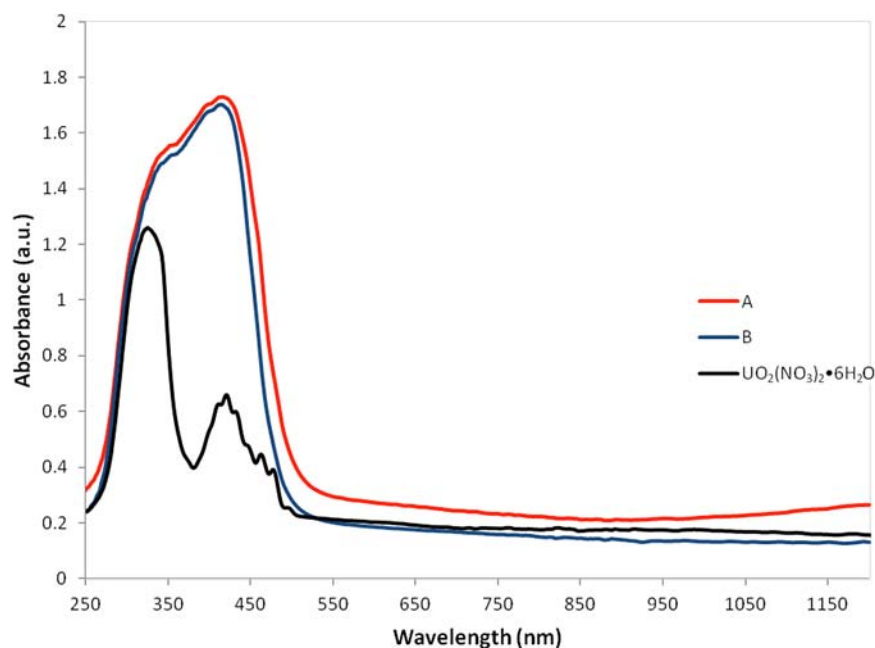
Figure 5. Absorption spectra of the two uranyl peroxide clusters (**A** and **B**), and uranyl nitrate hexahydrate.
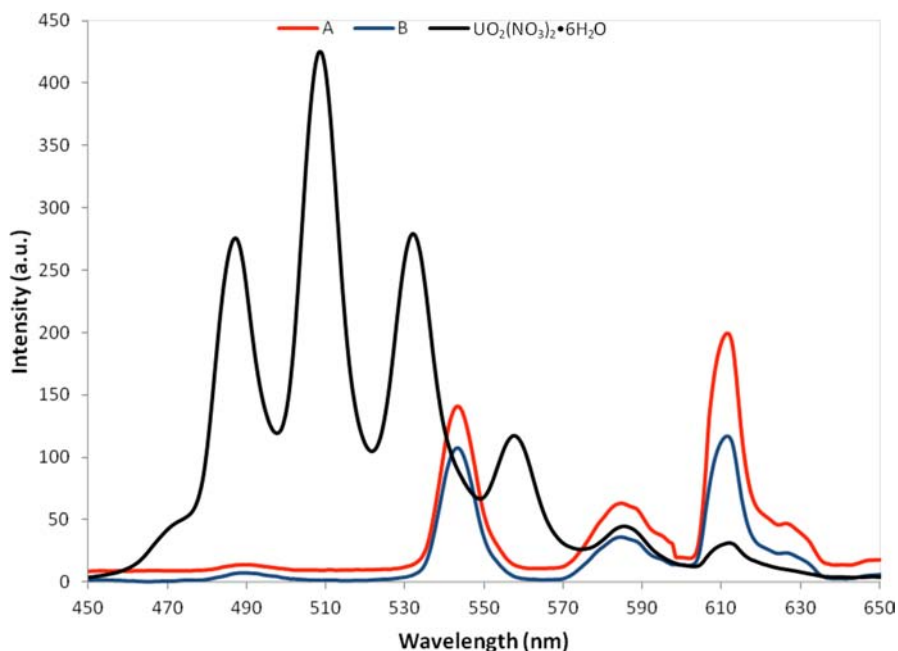

Figure 6. Luminescent spectra (365 nm excitation) of the two uranyl peroxide clusters (**A** and **B**), and the uranyl nitrate hexahydrate.

to the six-band emission pattern in the spectrum of the benchmark compound, $UO_2(NO_3)_2 \cdot 6H_2O$ (487, 509, 532, 558, 586, and 612).

The infrared bands from 700 to 775 cm^{-1}, as shown in Supporting Information, Figure S2, are dominated by the O–P–O bending, phenyl ring, and P–C stretching vibrations. The asymmetric and symmetric stretching modes of the uranyl cation, UO_2^{2+}, range from 879 to 977 cm^{-1}.[13,17,18,34] The group of peaks around 1040–1140 cm^{-1} is attributed to the P–O and P–O symmetric and asymmetric stretching modes of the phosphonates, while the bands around 1312–1445 cm^{-1} are assigned to phenyl ring stretching vibrations. The ν(C–O) of the carboxylate groups is located between 1590 and 1614 cm^{-1}

and the broad bands around 3139–3500 cm^{-1} are associated with free water molecules.[36,37]

■ DISCUSSION

The use of counterions and pH is very significant when constructing different topologies in uranyl peroxide clusters. Since similar counterions (Li$^+$ and K$^+$) were employed in the synthesis of the two cage clusters reported herein, the dominant role of either of the species is difficult to explain in the presence of the varied pH conditions and steric influence of the phenyl rings. Miro's studies based on density functional theory (DFT) calculations of counter cations indicate a strong propensity for square and pentagon topologies when Li and K cations are used, respectively.[49,50] However, we can presume that the low

ratio of K^+ to Li^+ used in the synthesis of **B** relative to **A** might have some effects in the isolation of clusters with topological squares. Only two of the oxygen atoms of the P−O group are employed in joining the pentagons and the 10-membered uranyl belt together in compound **A**. One of the oxygen atoms of the carboxylate group coordinates to each of the five uranyl cations of the pentagons. For compound **B**, all the oxygen atoms of the phosphonate along with one of the carboxylate groups, are involved in linking the uranyl cations. This is presumably responsible for the higher stability of **B** in solution. Attempts were made to incorporate transition metals in the 2-carboxyphenylphosphonate ligand, without success. Because of the high pH and the presence of H_2O_2, the expected differential binding preferences of the phosphonate and carboxylate groups around the uranium and the transition metals are not strictly based on Pearson's principle of hard/soft acid/base.[36,37,48] Moreover, the H_2O_2 group solubilizes uranium oxides, and its propensity for uranium is greater than transition metals.

Whereas the four and five-membered rings of uranyl hexagonal bipyramids found in **A** and **B** are common features of uranyl peroxide cage clusters, both clusters also contain novel units built from uranyl polyhedra. In cluster **A**, the belts consisting of 10 uranyl hexagonal bipyramids are reminiscent of the chains found in studtite, $[(UO_2)O_2(H_2O)_2]\cdot2H_2O$.[12] In both cases adjacent uranyl ions are bridged by bidentate peroxo groups that are in *trans* arrangements in their respective polyhedra, as also recently reported in four-membered belts in two clusters.[18] In contrast, most clusters are built from uranyl hexagonal bipyramids containing two peroxo ligands in a *cis* arrangement, including the belt-like unit consisting of 10 polyhedra in a cluster consisting of 20 uranyl polyhedra and 10 pyrophosphate units.[9] Cluster **B** is built from the well-known four-membered ring of uranyl hexagonal bipyramids, with each polyhedron containing two peroxo groups in a *cis* arrangement. The linkage of four such rings into a larger ring structure, consisting of 16 polyhedra, is novel. Note that adjacent four-membered rings in which the uranyl ions are all bridged by peroxo groups are linked through vertex-sharing only, which is another unusual feature of this cluster. Another fascinating feature that distinguishes these two structures from hybrid uranyl-organic cage clusters recently published by Burns and co-workers is the steric influence from the phenyl rings.[9,51] The phenyl rings are arranged on the outer periphery of the spherical core thus influencing the chelating and packing patterns.

In conclusion, the synthesis of the two hybrid uranyl cage clusters was achieved by connecting the uranyl moieties together using 2-carboxyphenylphosphonate ligands as secondary metal linkers. Nevertheless, the central question that will be addressed by the ongoing studies is whether we can incorporate 3d metal ions other than tungstometalate fragments to probe further the structural variation and electronic properties of such clusters.

ASSOCIATED CONTENT

Ⓢ Supporting Information

SAXS and IR spectra; and crystallographic data (CIF) of the two new clusters. This material is available free of charge via the Internet at http://pubs.acs.org.

AUTHOR INFORMATION

Corresponding Author

*E-mail: pburns@nd.edu.

REFERENCES

(1) Burns, P. C.; Kubatko, K.; Sigmon, G.; Fryer, B. J.; Gagnon, J. E.; Antonio, M. R.; Soderholm, L. *Angew. Chem., Int. Ed.* **2005**, *44*, 2135−2139.

(2) Soderholm, L.; Almond, P. M.; Skanthakumar, S.; Wilson, R. E.; Burns, P. C. *Angew. Chem., Int. Ed.* **2008**, *47*, 298−302.

(3) Forbes, T. Z.; McAlpin, J. G.; Murphy, R.; Burns, P. C. *Angew. Chem., Int. Ed.* **2008**, *47*, 2824−2827.

(4) Sigmon, G. E.; Unruh, D. K.; Ling, J.; Weaver, B.; Ward, M.; Pressprich, L.; Simonetti, A.; Burns, P. C. *Angew. Chem., Int. Ed.* **2009**, *48*, 2737−2740.

(5) Sigmon, G. E.; Weaver, B.; Kubatko, K.; Burns, P. C. *Inorg. Chem.* **2009**, *48*, 10907−10909.

(6) Sigmon, G. E.; Ling, J.; Unruh, D. K.; Moore-Shay, L.; Ward, M.; Weaver, B.; Burns, P. C. *J. Am. Chem. Soc.* **2009**, *131*, 16648−16649.

(7) Unruh, D. K.; Burtner, A.; Pressprich, L.; Sigmon, G. E.; Burns, P. C. *Dalton Trans.* **2010**, *39*, 5807−5813.

(8) Ling, J.; Wallace, C. M.; Szymanowski, J. E. S.; Burns, P. C. *Angew. Chem., Int. Ed.* **2010**, *49*, 7271−7273.

(9) Ling, J.; Qiu, J.; Sigmon, G. E.; Ward, M.; Szymanowski, J. E. S.; Burns, P. C. *J. Am. Chem. Soc.* **2010**, *132*, 13395−13402.

(10) Ling, J.; Qiu, J.; Szymanowski, J. E. S.; Burns, P. C. *Chem.—Eur. J.* **2011**, *17*, 2571−2574.

(11) Nyman, M.; Rodriguez, M. A.; Alam, T. M. *Eur. J. Inorg. Chem.* **2011**, 2197−2205.

(12) Burns, P. C. *Mineral. Mag.* **2011**, *75*, 1−25.

(13) Unruh, D. K.; Ling, J.; Qiu, J.; Pressprich, L.; Baranay, M.; Ward, M.; Burns, P. C. *Inorg. Chem.* **2011**, *50*, 5509−5516.

(14) Sigmon, G. E.; Burns, P. C. *J. Am. Chem. Soc.* **2011**, *133*, 9137−9139.

(15) Ling, J.; Ozga, M.; Stoffer, M.; Burns, P. C. *Dalton Trans.* **2012**, *41*, 7278−7284.

(16) Qiu, J.; Ling, J.; Sui, A.; Szymanowski, J. E. S.; Simonetti, A.; Burns, P. C. *J. Am. Chem. Soc.* **2012**, *134*, 1810−1816.

(17) Ling, J.; Qiu, J.; Burns, P. C. *Inorg. Chem.* **2012**, *51*, 2403−2408.

(18) Qiu, J.; Nguyen, K.; Jouffret, L.; Szymanowski, J. E. S.; Burns, P. C. *Inorg. Chem.* **2013**, *52*, 337−345.

(19) Armstrong, C. R.; Nyman, M.; Shvareva, T.; Sigmon, G. E.; Burns, P. C.; Navrotsky, A. *Proc. Natl. Acad. Sci. U. S. A.* **2012**, *109*, 1874−1877.

(20) Burns, P. C.; Ewing, R. C.; Navrotsky, A. *Science* **2012**, *335*, 1184−1188.

(21) Kim, K.; Pope, M. T. *J. Am. Chem. Soc.* **1999**, *121*, 8512−8517.

(22) Kim, K.; Pope, M. T. *J. Chem. Soc., Dalton Trans.* **2001**, 986−990.

(23) Kim, K.; Gaunt, A.; Pope, M. T. *J. Cluster Sci.* **2002**, *13*, 423−436.

(24) Gaunt, A. J.; May, I.; Helliwell, M.; Richardson, S. *J. Am. Chem. Soc.* **2002**, *124*, 13350−13351.

(25) Choppin, G. R.; Wall, D. E. *J. Radioanal. Nucl. Chem.* **2003**, *255*, 47−52.

(26) Gaunt, A. J.; May, I.; Copping, R.; Bhatt, A. I.; Collison, D.; Danny, F., O.; Travis, H., K.; Pope, M. T. *Dalton Trans.* **2003**, 3009−3014.

(27) Gaunt, A. J.; May, I.; Collison, D.; Holman, K. T.; Pope, M. T. *J. Mol. Struct.* **2003**, *656*, 101−106.

(28) Craciun, C.; Rusu, D.; Pop-Fanea, L.; Hossu, M.; Rusu, M.; David, L. *J. Radioanal. Nucl. Chem.* **2005**, *264*, 589−594.

7678

dx.doi.org/10.1021/ic4008262 | *Inorg. Chem.* 2013, 52, 7673−7679

(29) Khoshnavazi, R.; Eshtiagh-hossieni, H.; Alizadeh, M. H.; Pope, M. T. *Polyhedron* **2006**, *25*, 1921−1926.

(30) Antonio, M. R.; Chiang, M. *Inorg. Chem.* **2008**, *47*, 8278−8285.

(31) Mal, S. S.; Dickman, M. H.; Kortz, U. *Chem.—Eur. J.* **2008**, *14*, 9851−9855.

(32) Miró, P.; Ling, J.; Qiu, J.; Burns, P. C.; Gagliardi, L.; Cramer, C. J. *Inorg. Chem.* **2012**, *51*, 8784−8790.

(33) Nyman, M.; Burns, P. C. *Chem. Soc. Rev.* **2012**, *41*, 7354−7367.

(34) Adelani, P. O.; Albrecht-Schmitt, T. *Inorg. Chem.* **2011**, *50*, 12184−12191.

(35) Adelani, P. O.; Albrecht-Schmitt, T. E. *Angew. Chem., Int. Ed.* **2010**, *49*, 8909−8911.

(36) Adelani, P. O.; Albrecht-Schmitt, T. *Cryst. Growth Des.* **2011**, *11*, 4676−4683.

(37) Adelani, P. O.; Oliver, A. G.; Albrecht-Schmitt, T. *Inorg. Chem.* **2012**, *51*, 4885−4887.

(38) Sheldrick, G. M. *Acta Crystallogr.* **2008**, *A64*, 211.

(39) Fenn, J. B.; Mann, M.; Meng, C. K.; Wong, S. F.; Whitehouse, C. M. *Science* **1989**, *246*, 64−71.

(40) Burns, P. C.; Ewing, R. C.; Hawthorne, F. C. *Can. Mineral.* **1997**, *35*, 1551.

(41) Brese, N. E.; O'Keeffe, M. *Acta Crystallogr.* **1991**, *B47*, 192.

(42) Feigin, L. A.; Svergun, D. I. *Structure Analysis by Small-Angle X-Ray and Neutron Scattering*; Plenum Press: New York, 1987.

(43) Goff, G. S.; Brodnax, L. F.; Cisneros, M. R.; Peper, S. M.; Field, S. E.; Scott, B. L.; Runde, W. H. *Inorg. Chem.* **2008**, *47*, 1984−1990.

(44) Zanonato, P. L.; Di Bernardo, P.; Grenthe, I. *Dalton Trans.* **2012**, *41*, 3380−3386.

(45) Liu, G.; Beitz, J. V. In *The Chemistry of the Actinide and Transactinides Elements*; Morss, L. R., Edelstein, N. M., Fuger, J., Eds.; Springer: Heidelberg, Germany, 2006; p 2088.

(46) Adelani, P. O.; Albrecht-Schmitt, T. *Inorg. Chem.* **2010**, *49*, 5701−5705.

(47) Frisch, M.; Cahill, C. L. *Dalton Trans.* **2006**, 4679−4690.

(48) Adelani, P. O.; Oliver, A. G.; Albrecht-Schmitt, T. E. *Cryst. Growth Des.* **2011**, *11*, 3072−3080.

(49) Miro, P.; Pierrefixe, S.; Gicquel, M.; Gil, A.; Bo, C. *J. Am. Chem. Soc.* **2010**, *132*, 17787−17794.

(50) Miro, P.; Bo, C. *Inorg. Chem.* **2012**, *51*, 3840−3845.

(51) Liao, Z.; Ling, J.; Reinke, L. R.; Szymanowski, J. E. S.; Sigmon, G. E.; Burns, P. C. *Dalton Trans.* **2013**, *42*, 6793−6802.